

Supporting Information

A Novel Application of Dopants in Ion Mobility Spectrometry: Suppression of Fragment Ions of Citric Acid

Younes Valadbeigi^{†*}, Sahar Bayat[†], Vahideh Ilbeigi[‡],

[†]Department of Chemistry, Faculty of Science, Imam Khomeini International University, Qazvin, Iran.

[‡]TOF Tech. Pars Company, Isfahan Science & Technology Town, Isfahan, Iran.

(Y.V.) E-mail: valadbeigi@sci.ikiu.ac.ir. Tel: +98 28 3390 1367.

Content	page
Figure S1. Schematic representation of different parts of the IMS	S2
Figure S2. IMS spectra of citric acid at different temperatures of injection port	S3
Figure S3. IMS spectra of citric acid at different temperatures of the drift tube	S4
Figure S4. IMS spectra of citric acid in the presence of NH ₃ dopant	S5
Figure S5. Structures of the citric acid fragments and their protonated forms	S6
Figure S6. The optimized structures of NH ₄ ⁺ (H ₂ O) _n clusters	S7
Table S1. Calculated ΔH and ΔG values for hydration of NH ₄ ⁺	S7
Figure S7. Optimized structures of mono-, di-, and tri-hydrated form of CA.H ⁺	S8
Table S2. Calculated ΔH and ΔG values for hydration of CA.H ⁺	S9
Figure S8. Relative abundances for hydrated forms of NH ₄ ⁺ , CA.H ⁺ , and (CA-H) ⁺	S10
Figure S9. Structures of deprotonated forms of aconitic acid in gas phase	S11
Table S3. ΔH and ΔG values for protonation of the anionic reactant ions	S11
Figure S10. The optimized structures of hydrated forms of (CA-H) ⁻ in gas phase	S12
Table S4. The calculated ΔH and ΔG values for hydration of (CA-H) ⁻	S13
Figure S11. The optimized structures of hydrated forms of Cl ⁻ , Br ⁻ , and I ⁻	S13
Table S5. The calculated ΔH and ΔG values for hydration of Cl ⁻ , Br ⁻ , and I ⁻	S14
Figure S12. Relative abundances of (H ₂ O) _n Cl ⁻ , (H ₂ O) _n Br ⁻ , and (H ₂ O) _n I ⁻ ions	S14
Figure S13. Optimized structures for different isomers of CA.Cl ⁻ , CA.Br ⁻ , and CA.I ⁻	S15
Table S6. Calculated ΔH and ΔG values for formation of CA.Cl ⁻ , CA.Br ⁻ , and CA.I ⁻	S15
Figure S14. IMS spectra of citric acid with and without halomethane dopants	S16
Figure S15. Calibration curves for citric acid	S17
Figure S16. Manual preparation of fresh lemon juice	S18

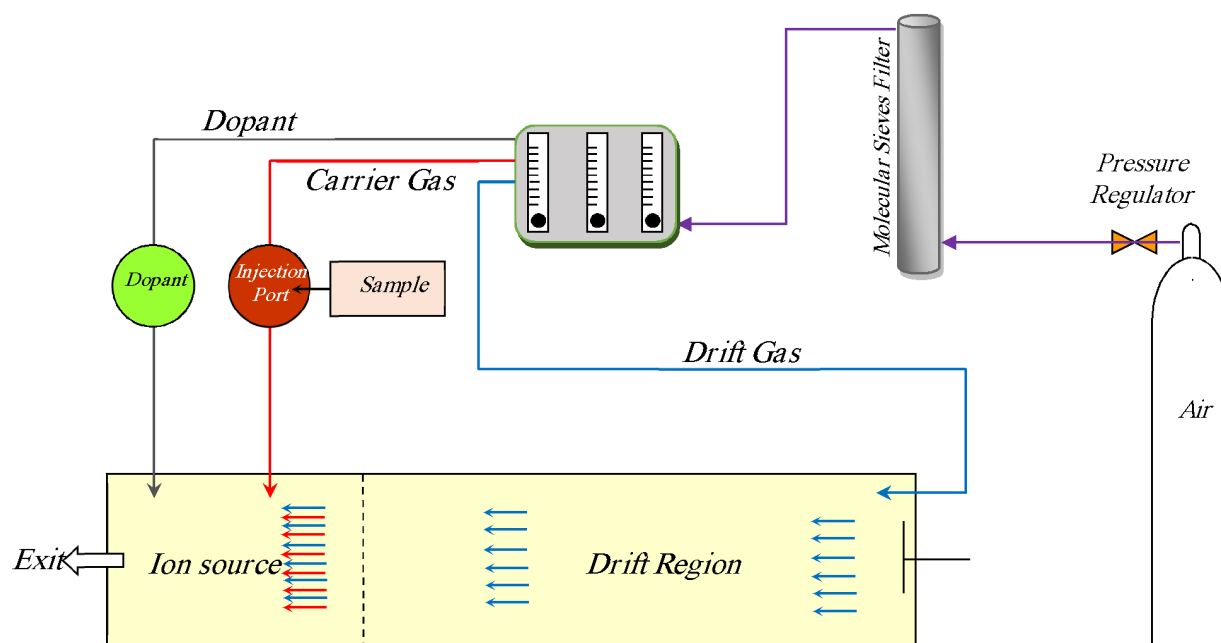


Figure S1. Schematic representation of different parts of the IMS used in this work and the paths of carrier, drift, and dopant gases.

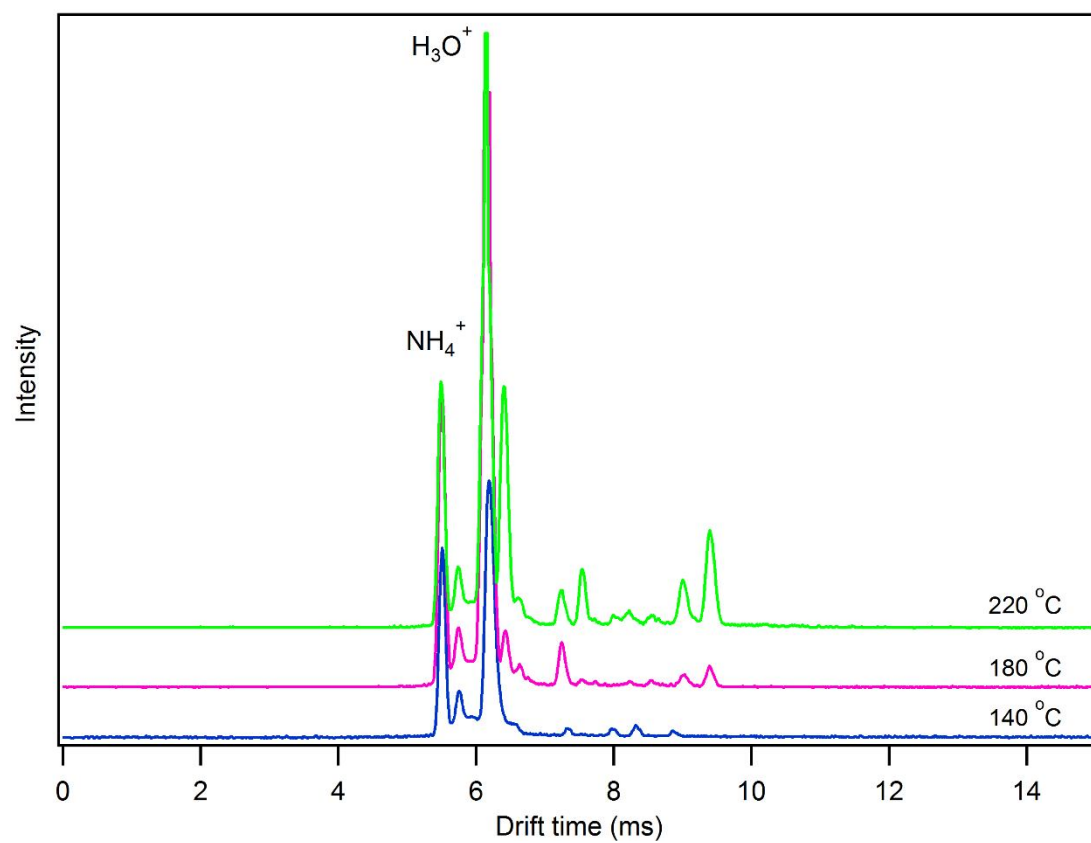


Figure S2. IMS spectra of citric acid (100 ppm) at different temperatures of the injection port with H_3O^+ as the main reactant ion RI. The drift tube temperature was 140 °C.

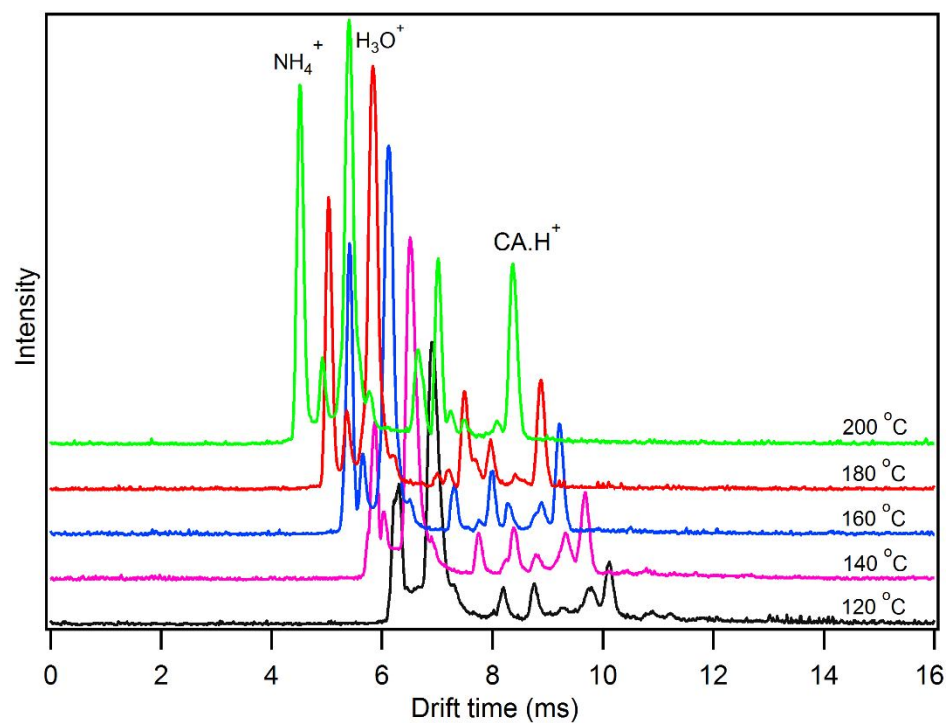


Figure S3. IMS spectra of citric acid at different temperatures of the drift tube in the absence of NH_3 dopant, i.e. the main reactant ion is H_3O^+ . The injection port temperature was 220 °C.

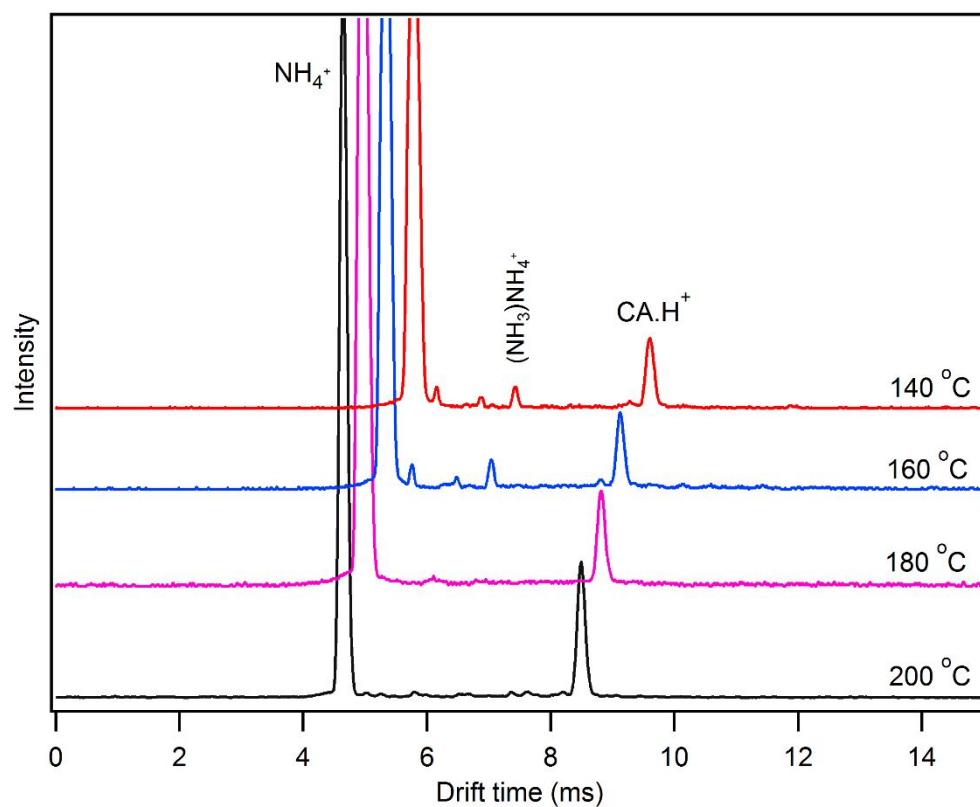


Figure S4. IMS spectra of citric acid (100 ppm) at different temperatures of the drift tube in the presence of NH_3 dopant. In this condition, the reactant ion is NH_4^+ . The injection port temperature was 220 °C.

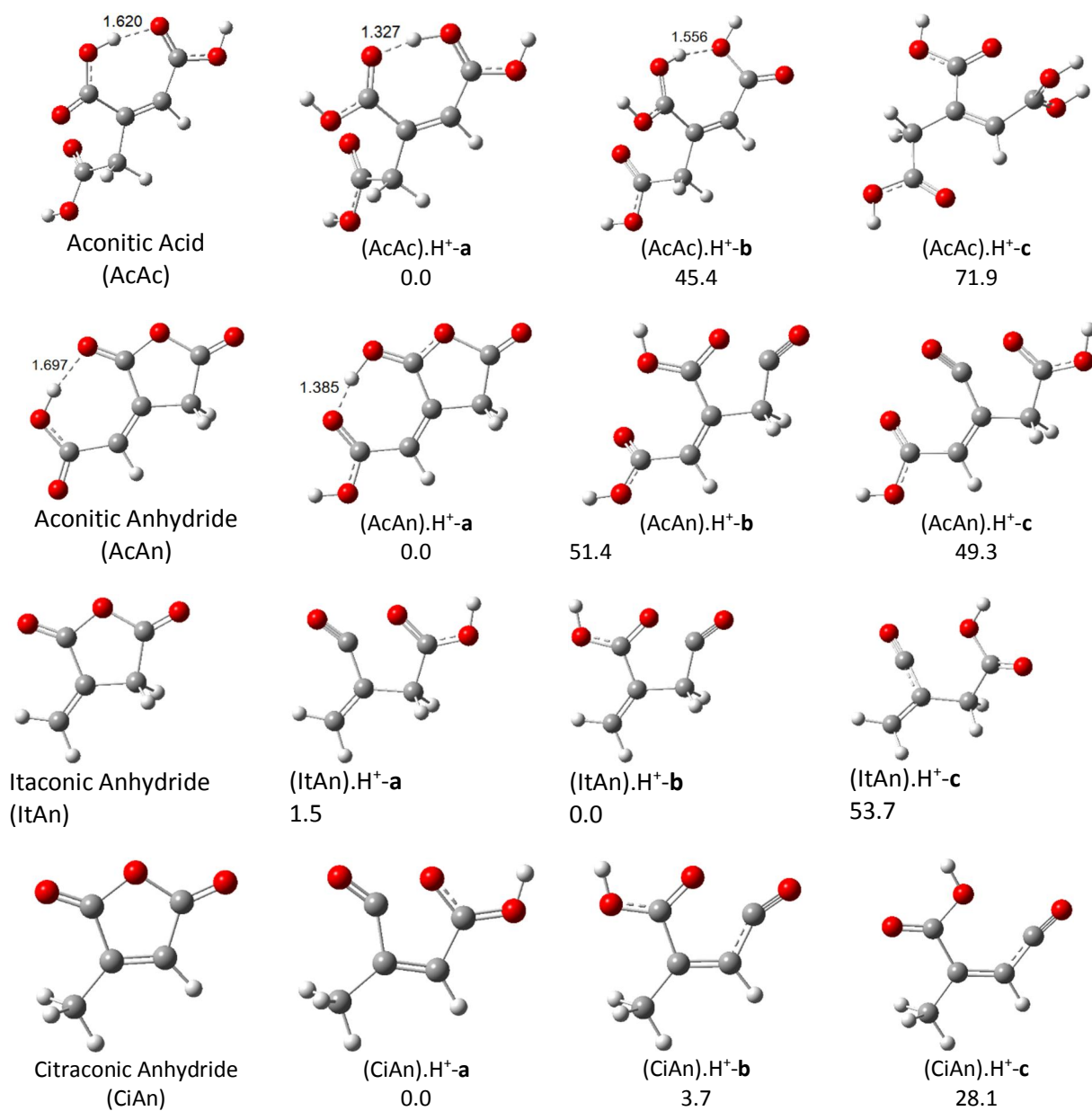


Figure S5. The optimized structures of the fragments of citric acid and their protonated forms. The relative energies and bond lengths are in kJ mol^{-1} and Å, respectively.

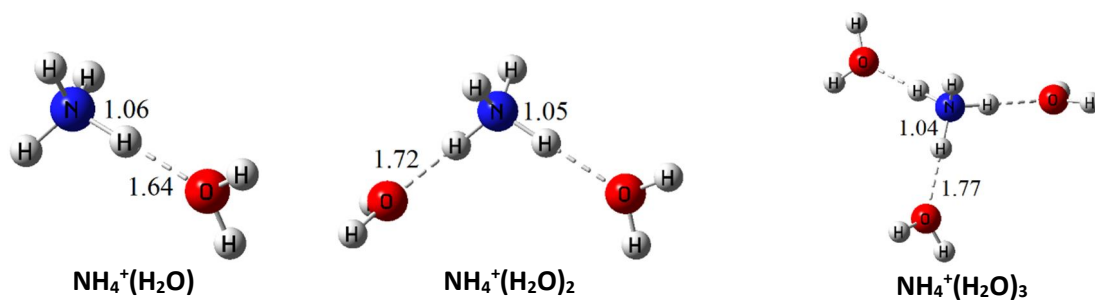


Figure S6. The optimized structures of $\text{NH}_4^+(\text{H}_2\text{O})_n$ clusters. The bond lengths are in Å.

Table S1. The calculated values of ΔH , ΔG and equilibrium constant (K) for formation of $\text{NH}_4^+(\text{H}_2\text{O})_n$ clusters in gas phase and at 298 K.

Hydration	ΔH (kJ mol ⁻¹)	ΔG (kJ mol ⁻¹)	K (1/atm)
$\text{NH}_4^+ + \text{H}_2\text{O} \rightarrow \text{NH}_4^+(\text{H}_2\text{O})$	-89.5	-50.1	5.9×10^8
$\text{NH}_4^+(\text{H}_2\text{O}) + \text{H}_2\text{O} \rightarrow \text{NH}_4^+(\text{H}_2\text{O})_2$	-66.9	-43.3	3.8×10^7
$\text{NH}_4^+(\text{H}_2\text{O})_2 + \text{H}_2\text{O} \rightarrow \text{NH}_4^+(\text{H}_2\text{O})_3$	-57.6	-23.3	1.2×10^4

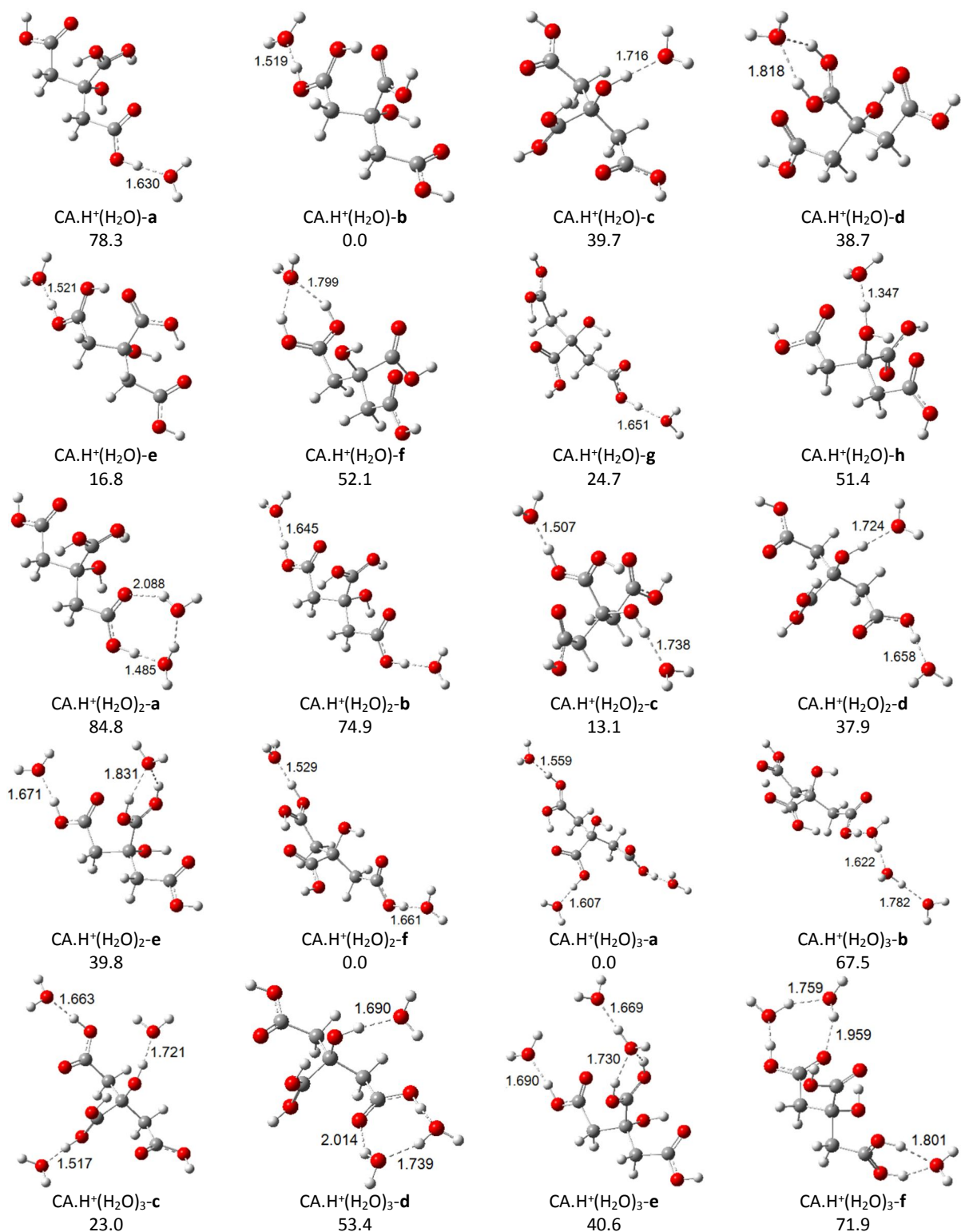


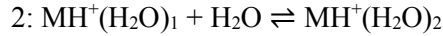
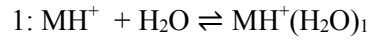
Figure S7. The optimized structures of mono-, di-, and tri-hydrated form of CA.H⁺ in gas phase. The relative energies and bond lengths are in kJ mol⁻¹ and Å, respectively.

Table S2. The calculated values of ΔH , ΔG and equilibrium constant (K) for hydration of $CA.H^+$ in gas phase and at 298 K.

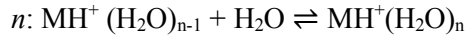
Hydration	ΔH (kJ mol ⁻¹)	ΔG (kJ mol ⁻¹)	K (1/atm)
$CA.H^+ + H_2O \rightarrow CA.H^+(H_2O)$	-75.9	-42.9	3.3×10^7
$CA.H^+(H_2O) + H_2O \rightarrow CA.H^+(H_2O)_2$	-64.8	-31.8	3.7×10^5
$CA.H^+(H_2O)_2 + H_2O \rightarrow CA.H^+(H_2O)_3$	-61.3	-27.4	6.3×10^4

S-1 hydration model

Relative abundances, Y_i , of $MH^+(H_2O)_i$ can be calculated from equilibrium constants for following consecutive reactions



.....



The equilibrium constant of each hydration reaction can be written as following

$$K_i = \frac{[MH^+(H_2O)_i]}{[MH^+(H_2O)_{i-1}]w} \quad (1)$$

Where w is water concentration. The equilibrium constant, K_i , can be computed from ΔG° of each hydration reaction

$$K_i = \exp(-\Delta G_i^\circ / RT) \quad (2)$$

where R is the gas constant and T is the absolute temperature.

Concentration of each ion can be obtained using equation (1)

$$MH^+(H_2O)_1 = [MH^+].w.K_1$$

$$MH^+(H_2O)_2 = [MH^+].w^2.K_1K_2$$

$$MH^+(H_2O)_j = [MH^+].w^j \prod_{i=1}^j K_i \quad (3)$$

The relative abundance for $MH^+(H_2O)_j$ is

$$Y_j = \frac{[\text{MH}^+(\text{H}_2\text{O})_j]}{\sum_{i=0}^{n_{\max}} [\text{MH}^+(\text{H}_2\text{O})_i]} \quad (4)$$

Where n_{\max} is the maximum number of water molecules in a $\text{MH}^+(\text{H}_2\text{O})_n$. n_{\max} was taken equal to 3 or 4.

Combination of equations (3) and (4) results in

$$Y_j = \frac{w^j \prod_{i=0}^j K_i}{\sum_{n=0}^{n_{\max}} w^n \prod_{i=0}^n K_i} \quad (5)$$

where $K_0=1$.

The van't Hoff equation was used to obtain the equilibrium constant, K_i , at the temperatures other than 25 °C (298 K):

$$\frac{d \ln K_i}{d(1/T)} = -\frac{\Delta H_i^\circ}{R} \quad (6)$$

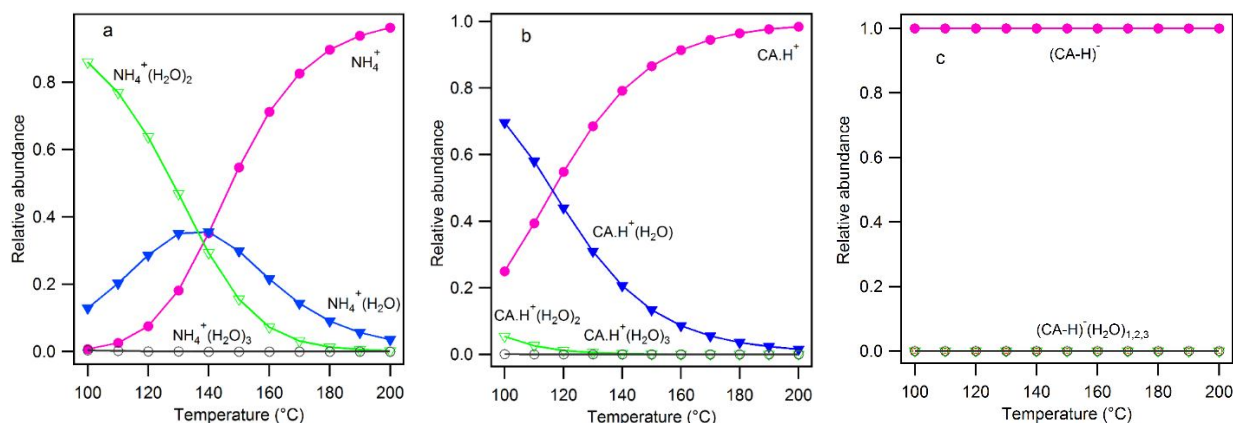


Figure S8. The calculated relative abundances for (a) $\text{NH}_4^+(\text{H}_2\text{O})_n$, (b) $\text{CA.H}^+(\text{H}_2\text{O})_n$, and (c) $(\text{CA-H})^-(\text{H}_2\text{O})_n$ in gas phase in the presence of 40 ppm water vapor.

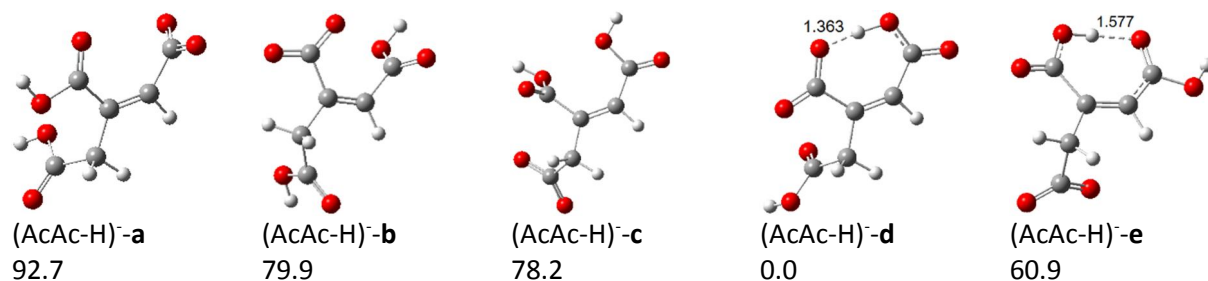


Figure S9. The optimized structures for different isomers of deprotonated form (conjugated bases) of aconitic acid in gas phase. The relative energies and bond lengths are in kJ mol^{-1} and Å, respectively.

Table S3. The calculated ΔH and ΔG values for protonation of the negative reactant ions (O_2^- , Cl^- , Br^- , I^-) and deprotonation of CA and its fragments in gas phase and at 298 K. The fragments with smaller deprotonation enthalpies are more acidic and deprotonated easier.

Protonation/deprotonation	ΔH (kJ mol^{-1})	ΔG (kJ mol^{-1})
$\text{O}_2^- + \text{H}^+ \rightarrow \text{HO}_2$	-1461.9	-1437.0
$\text{Cl}^- + \text{H}^+ \rightarrow \text{HCl}$	-1378.4	-1356.0
$\text{Br}^- + \text{H}^+ \rightarrow \text{HBr}$	-1341.2	-1319.2
$\text{I}^- + \text{H}^+ \rightarrow \text{HI}$	-1315.2	-1294.0
$\text{CA} \rightarrow (\text{CA-H})^- + \text{H}^+$	1278.8	1256.4
$\text{AcAn} \rightarrow (\text{AcAn-H})^- + \text{H}^+$	1355.3	1320.1
$\text{AcAc} \rightarrow (\text{AcAc-H})^- + \text{H}^+$	1303.8	1275.2
$\text{CH}_3\text{COOH} \rightarrow \text{CH}_3\text{COO}^- + \text{H}^+$	1446.1	1413.1
$\text{HCOOH} \rightarrow \text{HCOO}^- + \text{H}^+$	1426.4	1395.2

CA: Citric acid; AcAn: Aconitic anhydride; AcAc: Aconitic acid

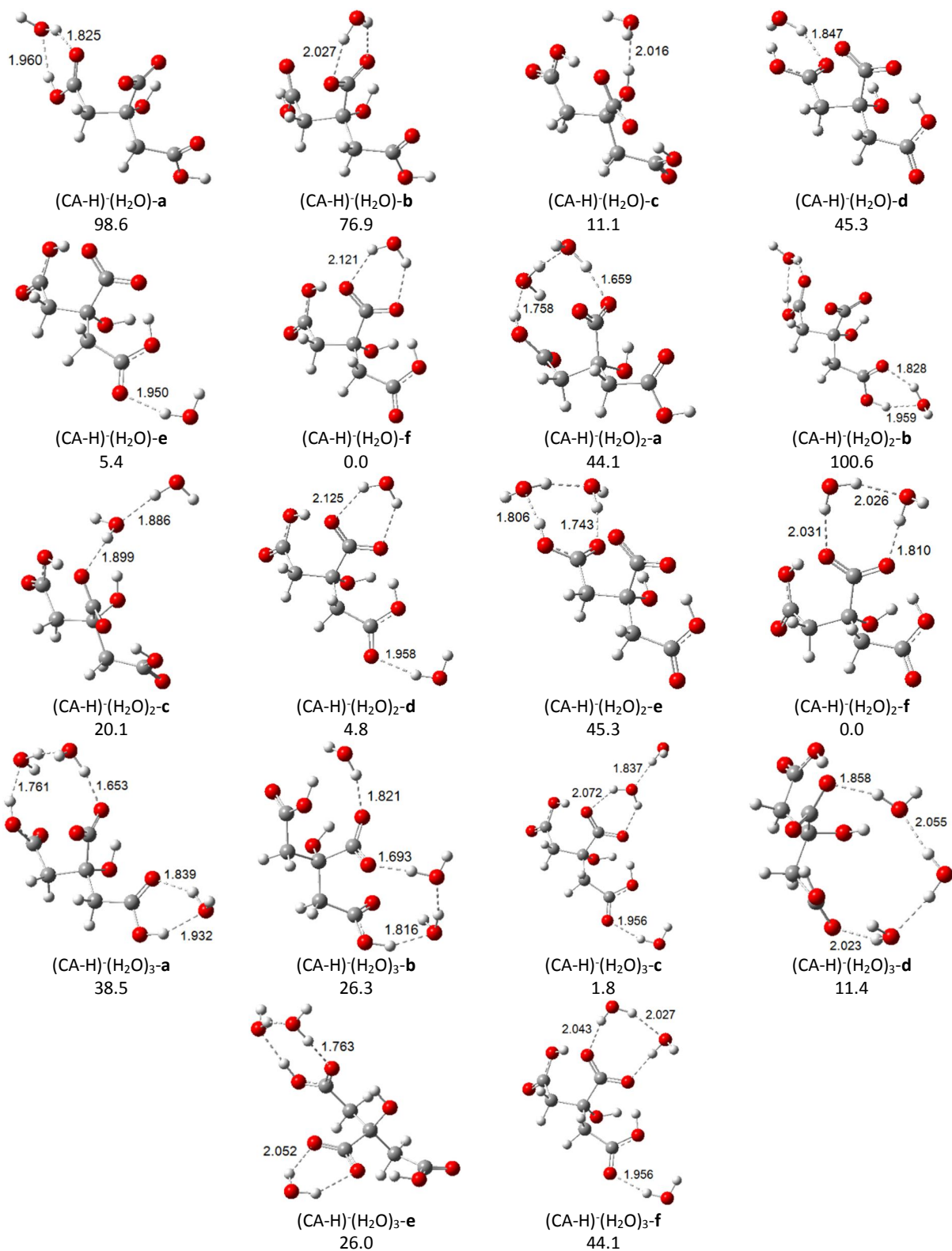


Figure S10. The optimized structures of mono-, di-, and tri-hydrated forms of (CA-H)⁻ in gas phase. The relative energies and bond lengths are in kJ mol⁻¹ and Å, respectively.

Table S4. The calculated values of ΔH , ΔG and equilibrium constant (K) for hydration of $(\text{CA-H})^-$ in gas phase and at 298 K.

Hydration	ΔH (kJ mol ⁻¹)	ΔG (kJ mol ⁻¹)	K (1/atm)
$(\text{CA-H})^- + \text{H}_2\text{O} \rightarrow (\text{CA-H})^-(\text{H}_2\text{O})$	-40.4	-6.6	1.4×10^1
$(\text{CA-H})^-(\text{H}_2\text{O}) + \text{H}_2\text{O} \rightarrow (\text{CA-H})^-(\text{H}_2\text{O})_2$	-36.7	1.2	6.1×10^{-1}
$(\text{CA-H})^-(\text{H}_2\text{O})_2 + \text{H}_2\text{O} \rightarrow (\text{CA-H})^-(\text{H}_2\text{O})_3$	-32.3	-0.4	1.2×10^0

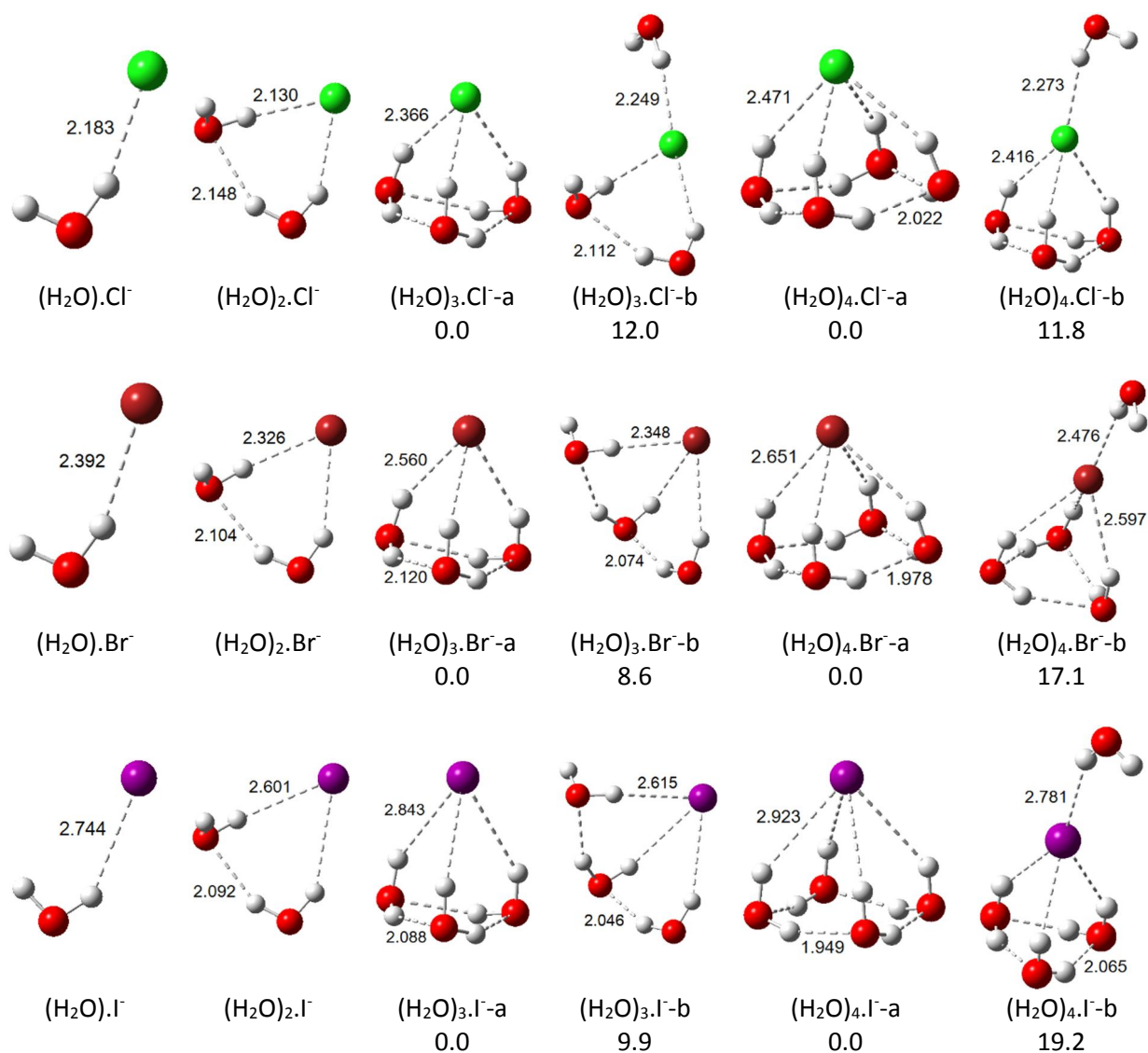


Figure S11. The optimized structures of hydrated forms of Cl^- , Br^- , and I^- with up to 4 water molecules in gas phase. The relative energies and hydrogen bond lengths are in kJ mol⁻¹ and Å, respectively.

Table S5. The calculated values of ΔH , ΔG and equilibrium constant (K) for hydration of Cl^- , Br^- , and I^- in gas phase and at 298 K.

Hydration	ΔH (kJ mol ⁻¹)	ΔG (kJ mol ⁻¹)	K (1/atm)
$\text{Cl}^- + \text{H}_2\text{O} \rightarrow (\text{H}_2\text{O})\text{Cl}^-$	-60.6 (61.5) ^a	-36.7 (-36.9) ^a	2.7×10^6
$(\text{H}_2\text{O})\text{Cl}^- + \text{H}_2\text{O} \rightarrow (\text{H}_2\text{O})_2\text{Cl}^-$	-53.1	-17.4	1.1×10^3
$(\text{H}_2\text{O})_2\text{Cl}^- + \text{H}_2\text{O} \rightarrow (\text{H}_2\text{O})_3\text{Cl}^-$	-52.4	-9.6	4.8×10^1
$(\text{H}_2\text{O})_3\text{Cl}^- + \text{H}_2\text{O} \rightarrow (\text{H}_2\text{O})_4\text{Cl}^-$	-49.2	-9.2	4.1×10^1
$\text{Br}^- + \text{H}_2\text{O} \rightarrow (\text{H}_2\text{O})\text{Br}^-$	-51.8 (49.0) ^a	-28.7 (-30.6)	1.1×10^5
$(\text{H}_2\text{O})\text{Br}^- + \text{H}_2\text{O} \rightarrow (\text{H}_2\text{O})_2\text{Br}^-$	-48.1	-12.5	1.6×10^2
$(\text{H}_2\text{O})_2\text{Br}^- + \text{H}_2\text{O} \rightarrow (\text{H}_2\text{O})_3\text{Br}^-$	-50.1	-7.2	1.8×10^1
$(\text{H}_2\text{O})_3\text{Br}^- + \text{H}_2\text{O} \rightarrow (\text{H}_2\text{O})_4\text{Br}^-$	-47.2	-4.5	6.2×10^0
$\text{I}^- + \text{H}_2\text{O} \rightarrow (\text{H}_2\text{O})\text{I}^-$	-43.1 ^a	-23.8 ^a	1.5×10^4
$(\text{H}_2\text{O})\text{I}^- + \text{H}_2\text{O} \rightarrow (\text{H}_2\text{O})_2\text{I}^-$	-39.7 ^a	-17.8 ^a	1.3×10^3
$(\text{H}_2\text{O})_2\text{I}^- + \text{H}_2\text{O} \rightarrow (\text{H}_2\text{O})_3\text{I}^-$	-38.5 ^a	-3.1 ^a	3.5×10^0
$(\text{H}_2\text{O})_3\text{I}^- + \text{H}_2\text{O} \rightarrow (\text{H}_2\text{O})_4\text{I}^-$	-38.5 ^a	-2.2 ^a	2.4×10^0

^a From: Hiraoka, K.; Mizuse, S.; Yamabe, S., Solvation of Halide Ions with H_2O and CH_3CN in the Gas Phase, *J. Phys. Chem.*, **1988**, 92, 13, 3943.

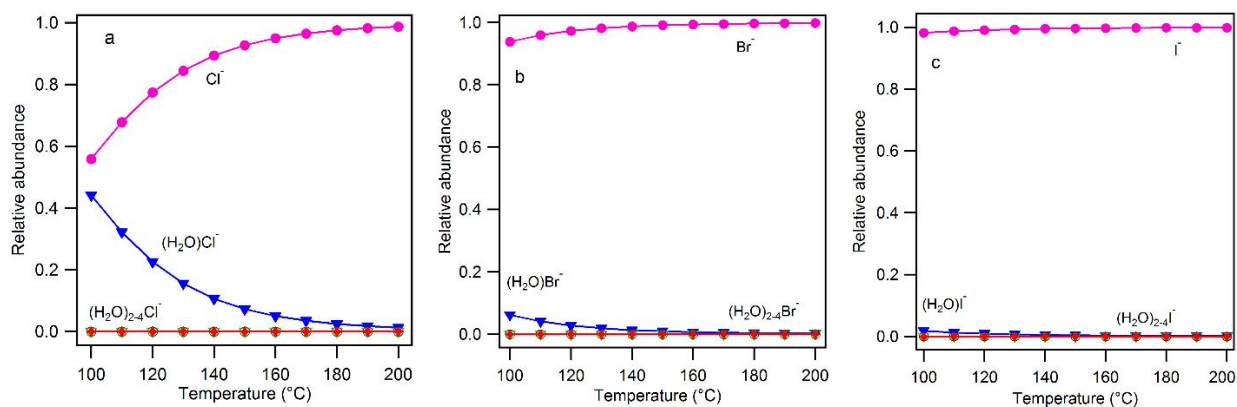


Figure S12. The calculated relative abundances for (a) $(\text{H}_2\text{O})_n\text{Cl}^-$, (b) $(\text{H}_2\text{O})_n\text{Br}^-$, and (c) $(\text{H}_2\text{O})_n\text{I}^-$ in gas phase in the presence of 40 ppm water vapor.

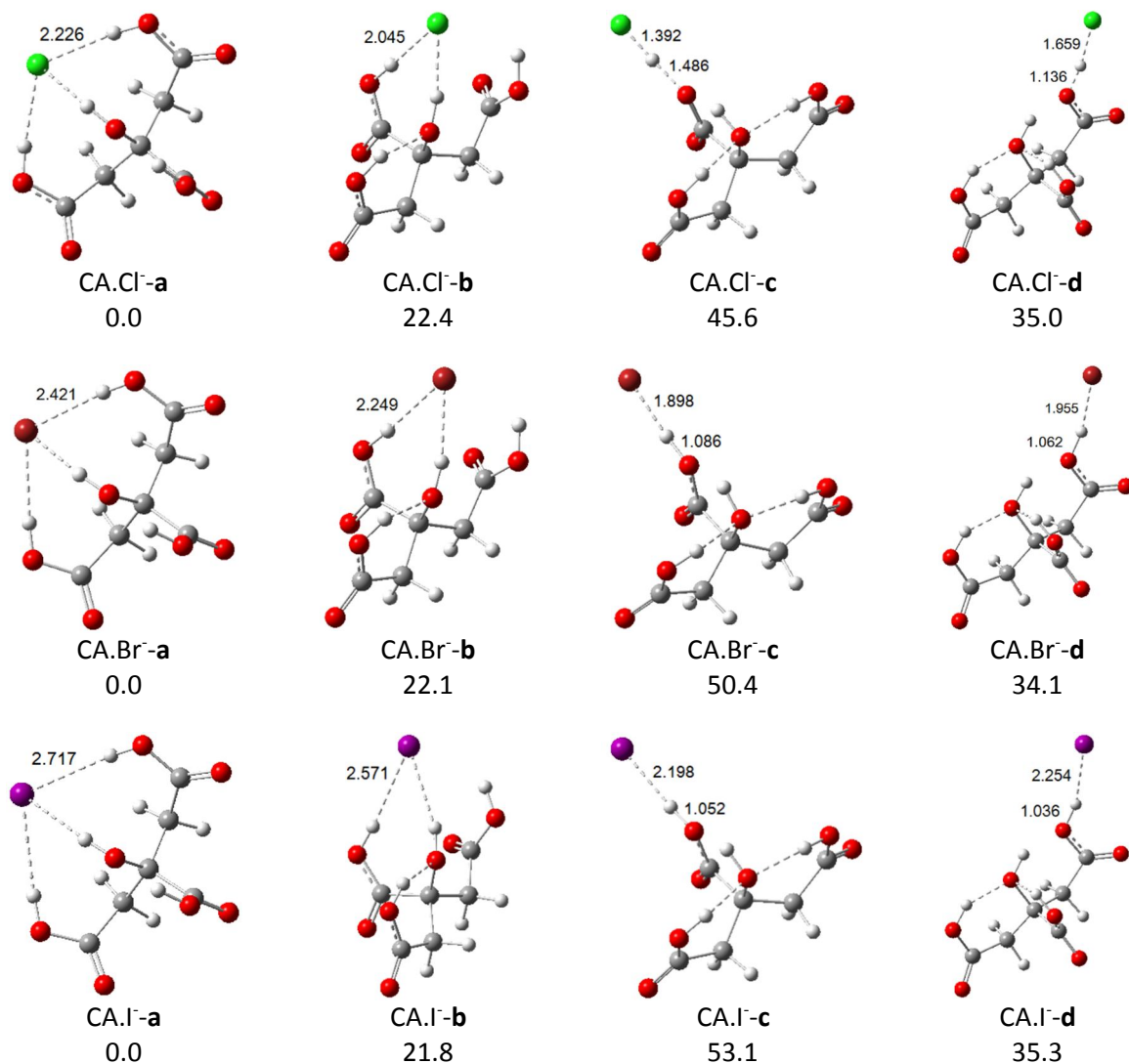


Figure S13. The optimized structures for different isomers of CA.Cl^- , CA.Br^- , and CA.I^- in gas phase. The relative energies and bond lengths are in kJ mol^{-1} and \AA , respectively.

Table S6. The calculated values of ΔH and ΔG for formation of the most stable isomers of CA.Cl^- , CA.Br^- , and CA.I^- in gas phase at 298 K.

Halide attachment	ΔH (kJ mol^{-1})	ΔG (kJ mol^{-1})
$\text{CA} + \text{Cl}^- \rightarrow \text{CA.Cl}^-$	-150.4	-110.7
$\text{CA} + \text{Br}^- \rightarrow \text{CA.Br}^-$	-143.6	-104.0
$\text{CA} + \text{I}^- \rightarrow \text{CA.I}^-$	-148.6	-111.4

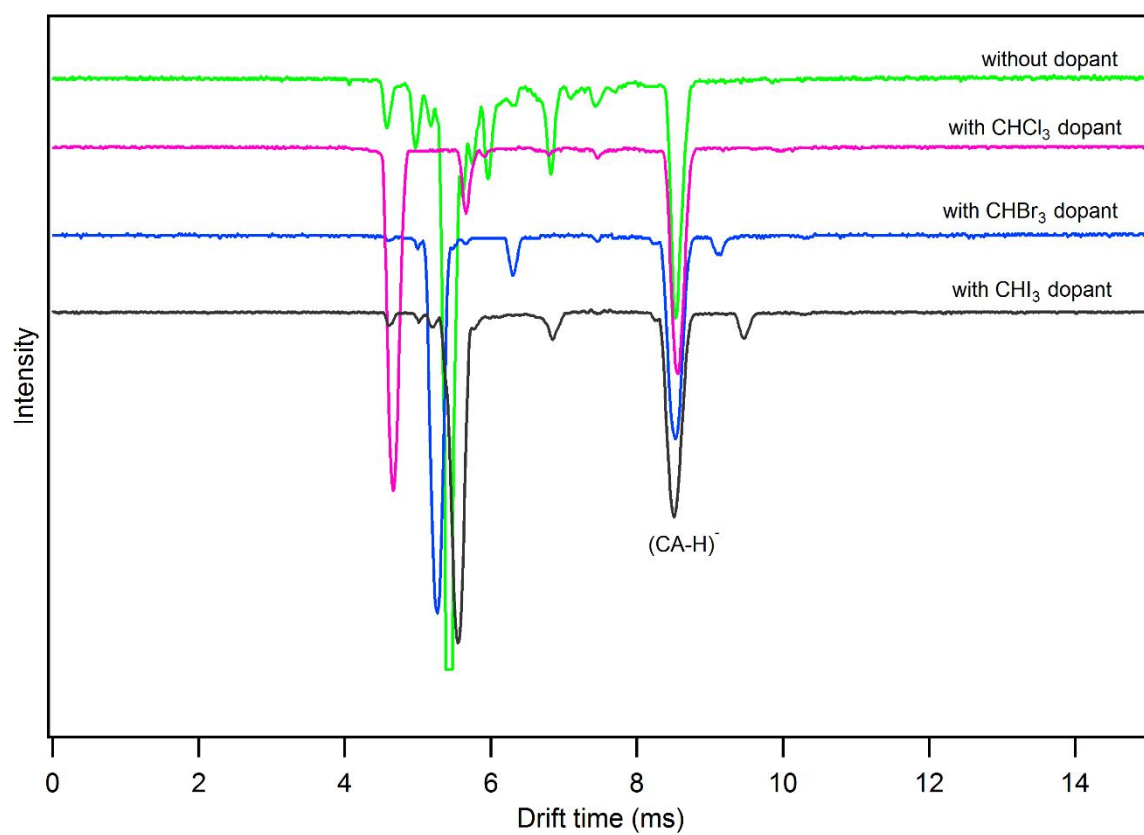


Figure S14. Comparison of IMS spectra of citric acid in negative mode with and without halomethane dopants (CHCl_3 , CHBr_3 , CHI_3) at drift tube temperature of 200 °C.

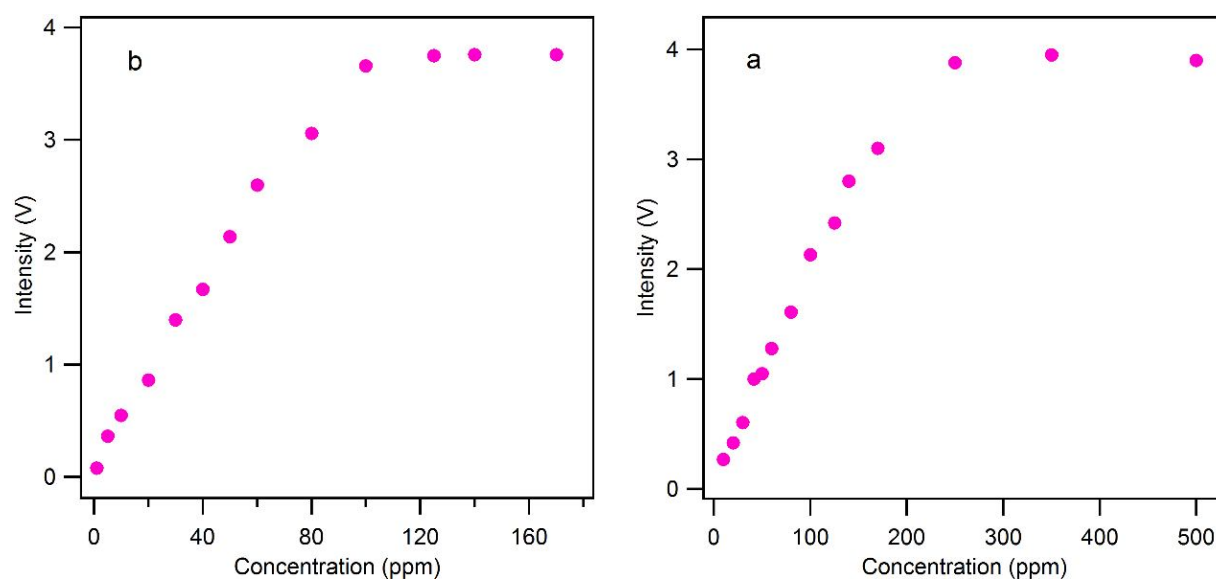


Figure S15. Calibration curves for citric acid obtained (a) in positive mode of IMS with NH_3 dopant and (b) in negative mode of IMS with CHCl_3 dopant.



Figure S16. Manual preparation of fresh lemon juice for direct injection into IMS.